

# Structural damage detection, localization, quantification for high-rise buildings under earthquake excitations based on machine learning and sub-structuring approach

Mohamed H. Abdelbarr<sup>1</sup>, ORCID (0000-0003-4558-7119), Yoshiki IKEDA<sup>2</sup>, Sami F. Masri<sup>3</sup>

<sup>1</sup>Structural Engineering Department, Faculty of Engineering Cairo University, Giza, Egypt

<sup>1</sup>Dar Al-Handasah, Giza, Egypt

<sup>2</sup>Earthquake Disasters Disaster Prevention Research Institute, Kyoto University Gokasyo, Uji, Kyoto, Japan

<sup>3</sup>Civil Engineering Department, University of Southern California, Los Angeles, CA, USA

email: abdelbarr@eng.cu.edu.eg, ikeda.yoshiki.6r@kyoto-u.ac.jp, masri@usc.edu

**ABSTRACT:** This work presents an evaluation of promising sub-structuring and machine learning SHM approaches suitable for high-rise buildings, based on real data from an 18-story steel-moment resisting framing building, tested at an E-Defense facility in Japan. This building is instrumented with a relatively dense set of sensor arrays and is subjected to different excitation levels until full collapse. The main contribution of this study is to demonstrate the practical feasibility of the proposed sub-structuring approach in conjunction with machine learning when relying on different levels of response measurements. The study assesses the accuracy and reliability of the estimates of the dominant modal features of the structure and can subsequently provide a probabilistic measure of confidence in the extent and location of changes/damage if an anomaly is detected, as well as the propagation of damage throughout the structure's life span. Due to the minimal computational resources needed to implement the sub-structuring approach, it is shown to be quite efficient for near-real-time applications where important structures need to be continuously monitored for sustainability as well as resiliency requirements.

**KEY WORDS:** Parametric identification; Nonparametric identification; Damage detection; Structural health monitoring; Condition assessment; High-rise building.

## 1 INTRODUCTION

Structural Health Monitoring (SHM) and condition assessment of high-rise buildings through vibration signature analysis have been extensively studied over time. SHM approaches for damage detection and condition assessment are generally classified into two main categories: local and global methods. Local methods focus on analyzing specific, limited areas of a structure using localized measurements. In contrast, global methods provide a comprehensive understanding of the system's condition by utilizing data from a distributed network of sensors. The selection of an appropriate method depends on several factors, including the problem's scope, the sensor network's configuration, the structural topology, and the level of detail required for the assessment.

Recent advancements in dense sensor networks, capable of collecting extensive data, have enabled the application of advanced data processing algorithms. These algorithms can effectively identify, localize, classify, and quantify changes or damages in civil infrastructure, including high-rise buildings, which are the primary focus of this study.

Prior to utilizing the identified vibrational signature of a structure for health monitoring, it is essential to comprehend the dynamic behavior modeling of high-rise buildings. This modeling is inherently complex due to various factors, including uncertainties in geometrical characteristics, material properties, nonlinear material behavior, foundation modeling, and soil effects. Therefore, integrating experimental and numerical data analysis enhances methods for identifying and localizing damage or changes within structural systems.

Extensive research in damage and change detection, as well as system identification for linear structural systems, has yielded numerous sophisticated global approaches based on vibration data analysis in both the time and frequency domains [13-15]. However, there is a notable lack of studies that leverage the topological features of the target structure to improve the detectability of minor changes. By employing appropriate substructuring techniques, these methods demonstrate superior sensitivity to small variations in the structural characteristics of the system under observation compared to global system identification methods.

In this study, one-third full-scale 18-story high-rise building was developed and instrumented with state-of-the-art instrumentation, installed on each floor and operated by E-Defense in Japan. This detailed testbed facilitated the creation of various data-driven, input-output, reduced-order models based on nonparametric identification approaches presented in [1-6], which have been successfully applied to both analytical and experimental data [7-8]. The approach discussed here does not require prior knowledge of the system characteristics (i.e., linear versus nonlinear) and is applicable to linear, nonlinear nonhysteretic, and hysteretic systems, without restrictions on the type of probing signal used for identification. However, it is limited to structures with chain-like topology, as will be subsequently explained in the study.

Several damage configurations in the building's lateral load-resisting system were investigated using data from base excitation dynamic tests performed on the building. The processes of damage detection, localization, and quantification were conducted by examining the variability in the primary features of the developed reduced-order models. It is important to note that in this study, the identification approaches were applied deterministically. The effects of variability in environmental or operational conditions, as well as uncertainties in modeling, measurement, and data analysis

processes, were not considered in the identified change-sensitive features (i.e., stiffness-like parameters and modal parameters) of the structures.

## 2 FORMULATION CHAIN-ID

Consider a multi-degree-of-freedom (MDOF) system with a chain-like topology, as illustrated in Figure 1. This system comprises  $n$  lumped masses, each with a magnitude  $m_i$ , subjected to base excitation and/or directly applied forces  $F_i$ . The lumped masses are interconnected by linear elements, whose restoring forces are primarily dependent on the relative displacement and velocity between the masses. The equations of motion for this system can be expressed as described by [9].

$$\ddot{x}_n + G^{(n)}(z_n, \dot{z}_n) = \frac{F_n}{m_n} \quad (1a)$$

$$G^{(n)}(z_n, \dot{z}_n) = \frac{F_n}{m_n} - \ddot{x}_n \quad (1b)$$

$$G^{(i)}(z_i, \dot{z}_i) = \frac{F_i}{m_i} - \ddot{x}_i + \frac{m_{i+1}}{m_i} G^{(i+1)}(z_{i+1}, \dot{z}_{i+1}) \quad (1c)$$

for  $i = n-1, n-2, \dots, 1$

where  $G^{(i)}(z_i, \dot{z}_i)$  is the mass-normalized restoring force function of the element connecting  $m_i$  and  $m_{i-1}$ ;  $x_i$  is the absolute acceleration of the mass  $m_i$ ;  $z_i$  the relative displacement between two consecutive masses; and  $\dot{z}_i$  the relative velocity between two consecutive masses. Equation (1) can be rewritten in more compact form as follows:

$$G^{(i)}(z_i, \dot{z}_i) = \sum_{j=i}^n \frac{F_j}{m_j} - \sum_{j=i}^n \bar{m}_{ij} \ddot{x}_j \quad (2)$$

where  $\bar{m}_{ij} = \frac{m_j}{m_i}$  represents the ratio between the lumped masses  $m_j$  and  $m_i$ . This approach assumes that the acceleration time responses  $\ddot{x}_i$  are available from observations, along with the applied forces  $F_i$  and/or the base excitation, as well as the values of the lumped masses  $m_i$ .

In addition, each of the estimated restoring force functions can be converted to a power series of the form

$$G^{(i)}(z_i, \dot{z}_i) = \sum_{q=0}^{q_{\max}} \sum_{r=0}^{r_{\max}} a_{qr}^{(i)} z_i^q \dot{z}_i^r \quad (3)$$

## 3 BUILDING DESCRIPTION AND CONFIGURATION

To evaluate the fundamental characteristics and validate the proposed methodology for earthquake responses and damage assessment in high-rise buildings, the data obtained from the shaking table test conducted at E-Defense in Japan are analyzed. E-Defense, operated by the National Research Institute for Earth Science and Disaster Resilience (NIED), is a 3D full-scale earthquake testing facility featuring the world's largest shaking table. The testbed is an 18-story moment-resisting frame structure, measuring 25.3 meters in height and weighing approximately 4179 kN, scaled down to one-third of a full-scale building [12]. Figure 2 and Figure 3 provide an overview and outline of the test specimen, respectively.

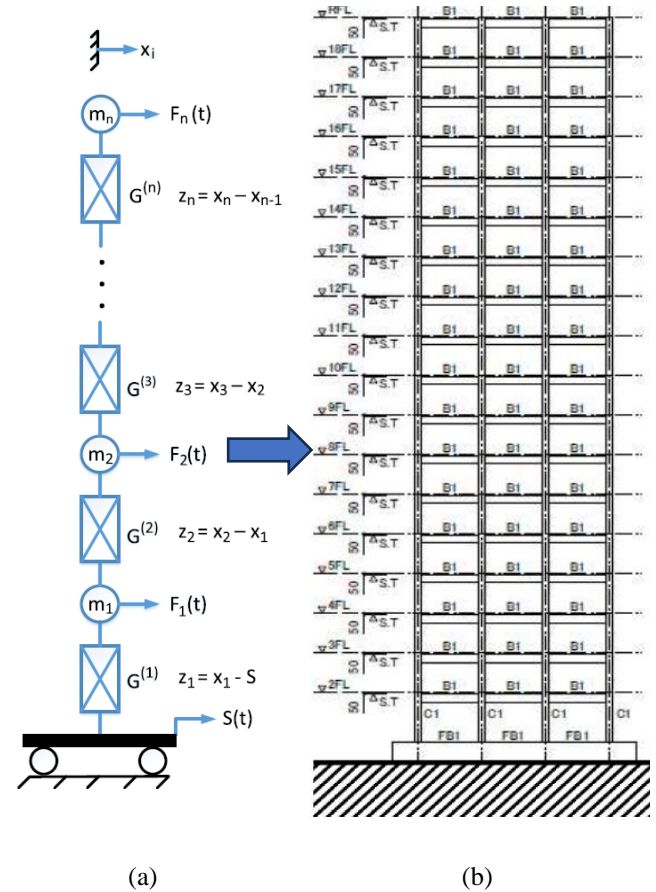


Figure 1. Modeling of the 18-story building used in this study: (a) reduced order representation (mathematical model), and (b) experimental setup.



Figure 2. Overview of testbed.

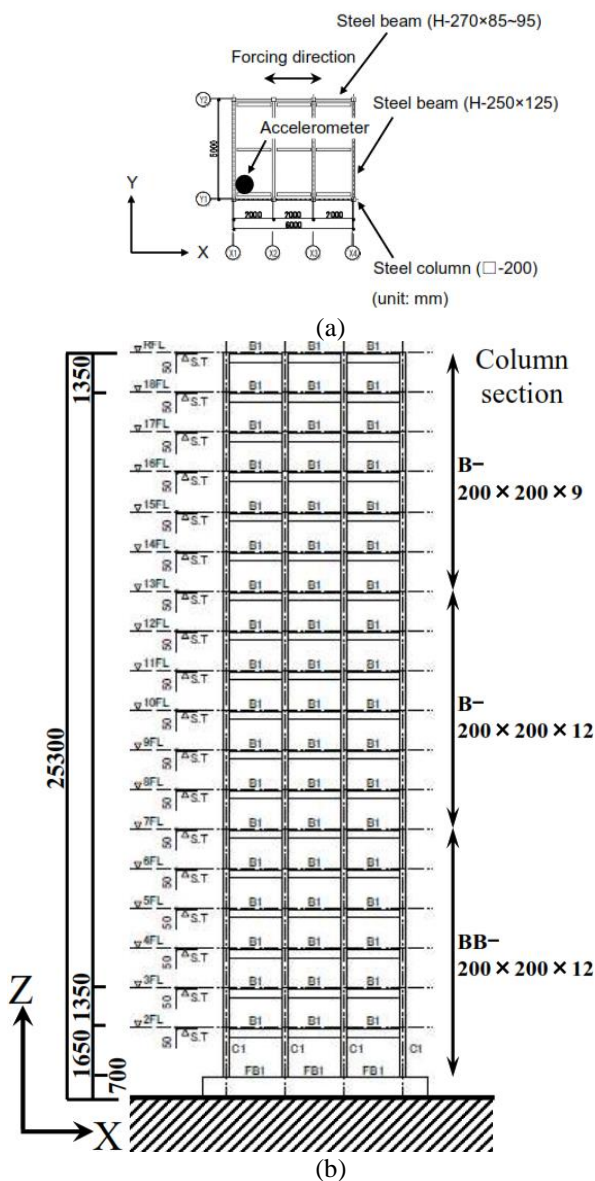


Figure 3. Outline of test specimen (a) floor plan and (b) structural framing elevation.

The floor plan measures 2000 mm by 3 spans in the longitudinal X-direction and 5000 mm by 1 span in the transverse Y-direction. The structure consists of moment-resisting frames with box-shaped steel columns measuring 200 mm by 200 mm, and H-shaped steel beams measuring 270 mm by 85-95 mm in the X-direction and 250 mm by 125 mm in the Y-direction. Servo-type three-axis accelerometers are installed at the corners of the X1 and Y1 bay on each floor of the test building. Measurement records from all floors and roof, totaling 18 accelerometers, are utilized for response estimation and damage evaluation in this study. The sensor signals are sampled at 200 Hz. The test specimen was subjected to a uniaxial excitation in the X-direction, with a first natural period of approximately 1.15 seconds in the X-direction.

The earthquake input motion is an artificially created Tokai, Nankai, and Tonankai consolidated-type earthquake occurring at the Nankai Trough, assumed to be recorded at Tsushima, Aichi Prefecture, Japan (Takahashi et al., 2013). Its peak ground acceleration (PGA) is about 300 cm/s<sup>2</sup>, with a velocity response spectrum value (pSv) of approximately 110 cm/s for periods between 0.8 and 10 seconds, and a duration of about 460 seconds. In the shaking table test, the input motion was scaled down to one-third of the original form to match the scale of the test specimen. The maximum excitation levels are set to various levels and applied to the test specimen multiple times.

Figure 4 shows the acceleration time history of the input motion to the testbed. Figure 5 illustrates the root mean square (RMS) for absolute acceleration, velocity, and displacement time-history for all floors in x-direction for the testbed. Figure 6 shows computed for relative displacement, relative velocity, and restoring force time-history for all floors in x-direction based on Equations 1 and 2.

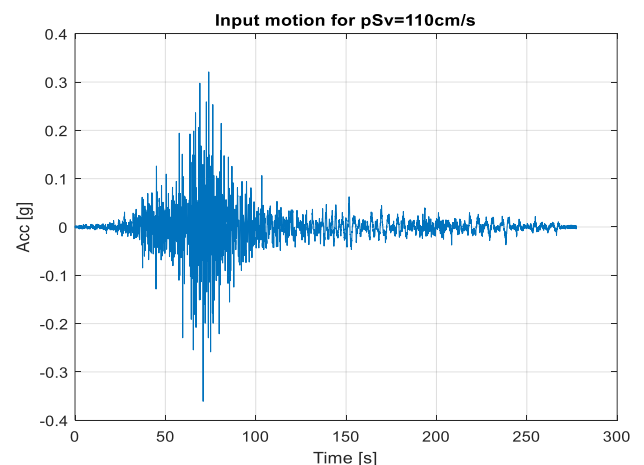


Figure 4. Acceleration time history of input motion for pSv=110cm/s.



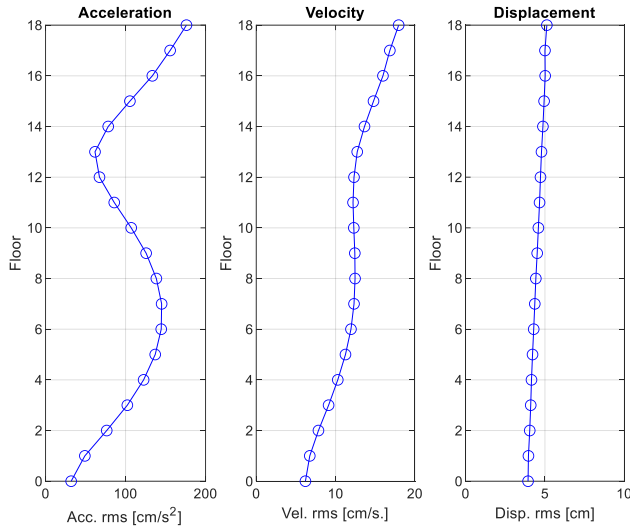


Figure 5. Computed RMS for absolute acceleration, velocity, and displacement time-history for all floors in x-direction.

## 4 DAMAGE IDENTIFICATION

### 4.1 Sample Data Processing

The acceleration responses were acquired from each floor of the testbed at a sampling frequency of 200 Hz. Corresponding velocity and displacement time histories were obtained through digital signal processing and numerical integration. Additionally, it was assumed that the building slabs were rigid; therefore, the available acceleration measurements corresponded to the acceleration response of the structure at each slab's geometric center. It is important to note that the experimental data contains all sources of measured uncertainty as the data was recorded from a real physical structure. To create a set of data, the time-history record for each structural state/configuration was partitioned into 40 ensembles with 20% overlap (i.e., in a sliding window of 30-second duration). Each ensemble includes more than five fundamental periods of the system.

### 4.2 Decomposition Approach

The building structure was utilized to demonstrate the results of implementing the proposed approach detailed in the second section of the paper, aimed at constructing a reduced-order model for the building structure. The decomposition approach for restoring force identification was executed using a third-order polynomial in both normalized variables  $z_i$  and  $\dot{z}_i$  for all floors in the building structure. The selection of a third-order polynomial was intentional to illustrate that the nonparametric identification approach discussed is capable of autonomously detecting whether the system is linear or nonlinear.

Once the relative displacements and velocities were computed, the ChainID identification approach was applied to develop the associated nonparametric representation for each floor in the 18-story building structure by calculating the corresponding restoring force coefficients for each floor in the reference structural configuration. Figure 7 illustrates sample time-history plots for the relative displacement  $z_i$ , relative velocity  $\dot{z}_i$  and measured mass normalized restoring force  $G^{(14)}$  between the 14<sup>th</sup> and 13<sup>th</sup> floors, in the x-directions.

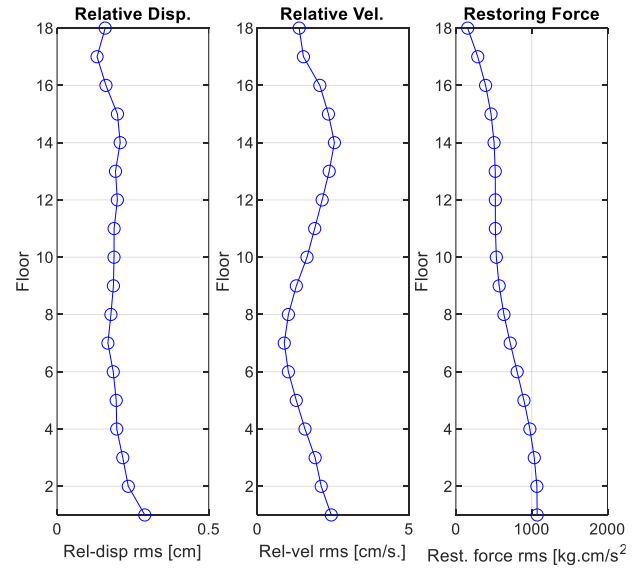


Figure 6. Computed RMS for relative displacement, relative velocity, and restoring force time-history for all floors in x-direction.

The analysis of the identified restoring force coefficients (i.e., power series coefficients  $a_{qr}^{(i)}$  for all building floors indicated that the linear term associated with relative displacements in the nonparametric representation (i.e.,  $a_{10}^{(i)}$ ) had the most significant contribution to the restoring force  $G^{(i)}$ , while the nonlinear terms were negligible. Figure 8 summarizes the identified mean of mass-normalized stiffness-like coefficient ( $a_{10}^{(i)}$ ) for all floors in x-direction.

For brevity, only the identification results computed for the 14<sup>th</sup> floor will be presented and discussed in this section. The power series coefficients  $a_{qr}^{(14)}$  of the nonparametric representation for the 14<sup>th</sup> floor are summarized in Table 1. It is evident that the mass-normalized stiffness-like coefficient  $a_{10}^{(14)}$  was the dominant term in the nonparametric representation.

It can be seen from Table 1 that only the linear terms in the identified model are found to be dominant. However, for the 1<sup>st</sup> floor, nonlinear terms had more contribution due to the presence of plastic hinges at the damaged location, as will be discussed in the upcoming section. It is important to mention that the same control parameters were used to perform the analysis without making any assumptions regarding the presence or absence of nonlinear response features. Figure 9 illustrates the time-history of the measured (experimental data) and reconstructed (after the application of ChainID approach) mass-normalized restoring forces for the 14<sup>th</sup> floor in the reference configuration in the x-direction. The two curves are essentially identical, indicating that the reduced-order model was able to replicate the dominant behavior of the 14<sup>th</sup> floor.

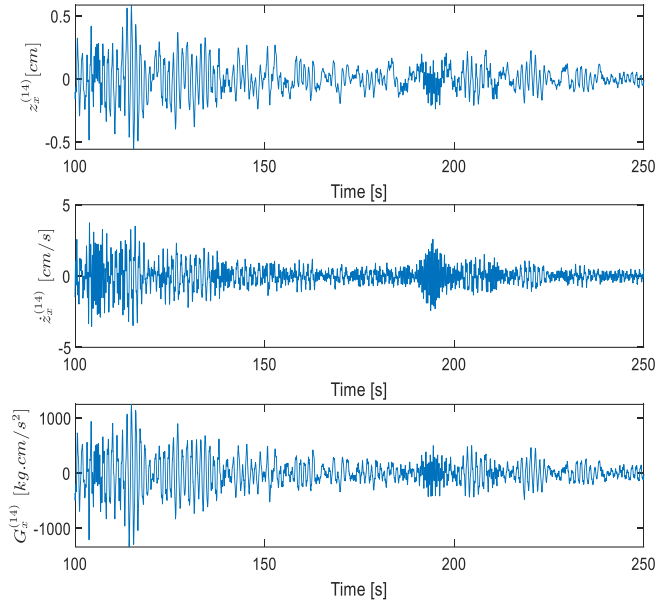


Figure 7. Sample relative displacement  $z_i$  and relative velocity  $\dot{z}_i$  computed between the 14<sup>th</sup> and 13<sup>th</sup> floors. The third row presents the measured restoring force time-history for element  $G^{(14)}$ .

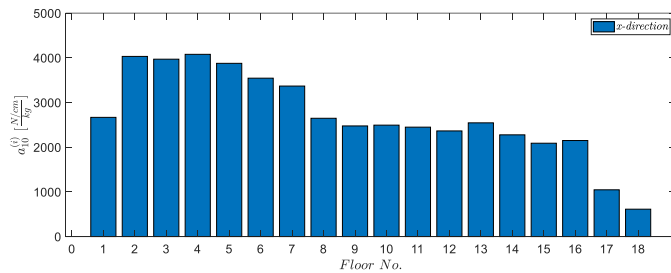


Figure 8. Identified mean of mass-normalized stiffness-like coefficient ( $a_{10}^{(i)}$ ) for all floors in x-direction.

Table 1. Identified mass-normalized restoring force coefficients  $a_{qr}^{(14)}$  for the 14th floor.

q\r	X-direction			
	0	1	2	3
0	0.00	2.10	-0.13	0.00
1	2276	0.90	0.20	0.00
2	12.30	3.20	0.00	0.00
3	78.00	0.00	0.00	0.00

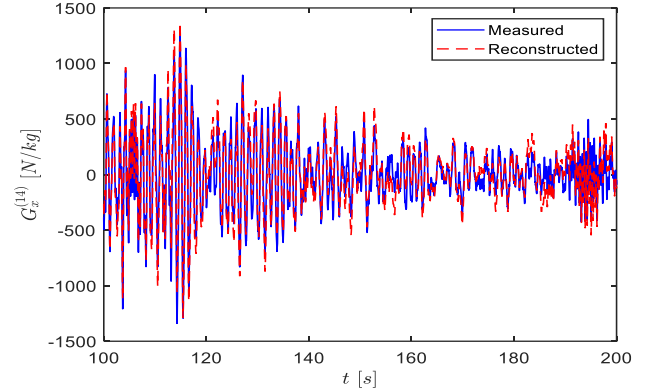


Figure 9. Comparison of measured and estimated restoring forces  $G^{(i)}$  for 14<sup>th</sup> floor in x-direction. Solid lines correspond to measured restoring force time-history; and dotted lines correspond to reconstructed restoring force time-history.

### 4.3 Damage Detection

To visualize the primary dynamic features of the system, the experimental phase plots (blue line) and the reduced-order representation using the ChainID approach (dotted red line) as well as the restoring force surface, are compared for the 14<sup>th</sup> and 1<sup>st</sup> floors, as shown in Figure 10.

It can be seen from Figure 10 (a), the reconstructed reduced-order model successfully captured the dominant linear dynamic characteristics of the 14<sup>th</sup> floor. Similarly, the reconstructed restoring force surface is planar, despite the use of a third-order expansion in both state variables (i.e., relative displacement and relative velocity) to characterize the dynamics of the 14<sup>th</sup> floor. The actual restoring force measurements are plotted as a point cloud, as shown in the second row of Figure 10 (a).

It is important to note that the data set under discussion was obtained from the testbed, where significant damage was observed on the 1<sup>st</sup> floor. This damage was characterized by the formation of plastic hinges at several columns, indicating a localized failure mechanism. The presence of plastic hinges suggests that the columns experienced substantial stress and deformation, leading to a reduction in their load-bearing capacity. This observation is crucial for understanding the structural behavior and integrity of the building under dynamic loading conditions.

The presence of plastic hinges and damage in the columns of the 1<sup>st</sup> floor led to the anticipated nonlinear behavior of the floor. This nonlinear response is indicative of the significant stress and deformation experienced by the columns, restoring forces  $G^{(i)}$  versus relative displacements  $z_i$  for the 1<sup>st</sup> floor and corresponding estimated restoring force surface for the 1<sup>st</sup> floor in the x-direction. In the first row, solid lines correspond to phase plot for the measured restoring force, and dotted lines correspond to reconstructed restoring force. In second row, actual restoring force measurements were plotted as a point cloud, which compromised their structural integrity and load-bearing capacity. The formation of plastic hinges is a critical factor in understanding the overall dynamic performance and failure mechanisms of the building under applied loads.

Figure 10(b) illustrates that the presence of nonlinearity can be visually inspected from the reconstructed restoring force for the 1<sup>st</sup> floor ( $G^{(1)}$ ), compared to the restoring force plot for the 14<sup>th</sup> ( $G^{(14)}$ ) floor under the same excitation. The effects of the nonlinear element in the response of the 1<sup>st</sup> floor are evident in both phase plots of the restoring force when compared to the reference condition, as shown in Figure 10 (b). In the phase plot of restoring force and relative displacement, the change in the restoring force slope indicates a pinching effect in the introduced nonlinearity. This pinching effect is observed on both sides of the restoring force, as the introduced damage is symmetric.

Additionally, a nonlinear effect in the restoring force surface can be seen in the plot of restoring force versus relative displacement and relative velocity, which is a typical signature of damage features. It is important to note that the nonparametric reduced-order representation using the ChainID approach successfully captured the dominant features of the dynamics at the correct location within the modules where the damage elements occurred. This demonstrates the effectiveness of the ChainID approach in accurately identifying and characterizing the nonlinear dynamic behavior resulting from structural damage.

## 5 MODAL IDENTIFICATION USING GLOBAL IDENTIFICATION

In addition to the local identification of the dynamic properties of each floor in the building, the modal identification (i.e., modal parameters) of the building was accomplished using the identified restoring force coefficients, as detailed in [10]. The estimated modal parameters were compared to those directly identified by implementing the natural excitation technique (NExT) in combination with the eigensystem realization algorithm (ERA) [11] a global identification technique.

The estimated values for the modal parameters (i.e., natural frequencies and damping ratios) for the first four mode shapes in x- directions are summarized in Table 2. It is noteworthy that the natural frequencies estimated from the reduced-order models developed in this study closely align with those computed using the NExT/ERA approach. As shown in Table 2, the estimated damping ratios computed using the two different approaches are similar for the first mode shape; however, damping was not identified for the remaining modes. This discrepancy is attributed to the varying contributions of the different modal constituents in characterizing the restoring forces.

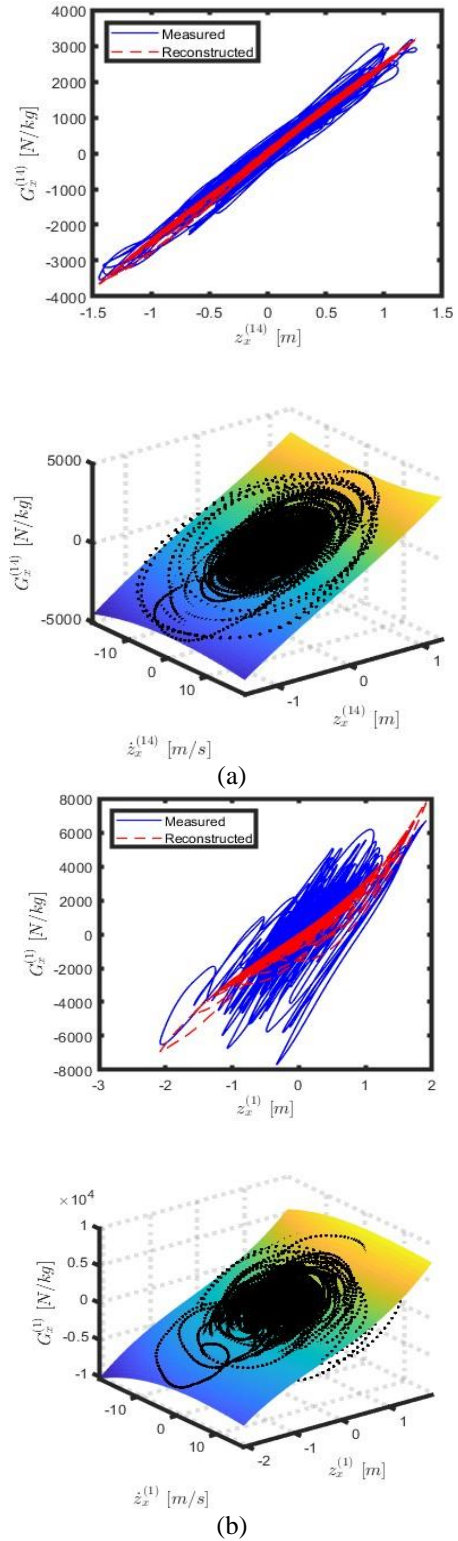


Figure 10. Phase plot of (a) restoring forces  $G^{(i)}$  versus relative displacements  $z_i$  for 14<sup>th</sup> floor and corresponding estimated restoring force surface for 14<sup>th</sup> floor in x-direction; and (b) restoring forces  $G^{(i)}$  versus relative displacements  $z_i$  for the 1<sup>st</sup> floor and corresponding estimated restoring force surface for the 1<sup>st</sup> floor in x-direction. In first row, solid lines correspond to phase plot for measured restoring force, and dotted lines correspond to reconstructed restoring force. In second row, actual restoring force measurements were plotted as a point cloud.

Table 2. Summary of natural frequencies and damping ratios for the first four lateral modes in the x-directions of the 18-story building structure, identified from the reduced-order model developed using ChainID and NExT/ERA approaches.

Mode	Chain ID		NExT/ERA	
	$\omega$ [Hz]	$\zeta$ [%]	$\omega$ [Hz]	$\zeta$ [%]
1 <sup>st</sup> mode	0.38	1.78	0.48	1.75
2 <sup>nd</sup> mode	0.81	-	0.82	0.40
3 <sup>rd</sup> mode	1.19	-	1.16	0.20
4 <sup>th</sup> mode	1.65	-	1.79	1.00

## 6 SUMMARY AND CONCLUSIONS

In this study, a one-third full-scale model of an 18-story high-rise building, developed under the E-Defense project, was constructed and instrumented to investigate the damage on individual floors. Sample results from these damage scenario models were used to evaluate the effectiveness and reliability of employing reduced-order models to detect, locate, and quantify changes or damages in a physical building structure.

Input-output data from the 18-story building under base excitation were used to develop reduced-order models for different floors. Two approaches were implemented: the nonparametric chain-like system identification approach (ChainID), which is the focus of this study, and a global identification approach (NExT/ERA). The results demonstrated that significant changes identified in the reconstructed restoring forces of the reduced-order models built using the ChainID approach could be correlated to the presence and location of the actual physical changes or damages, even in the presence of modeling, measurement, and data processing errors.

The initial findings of this study demonstrate that the structural health monitoring methodology presented is capable of accurately detecting, locating, and quantifying structural changes or damage in monitored systems, provided the necessary data set is available.

The presented work is part of an ongoing effort. Future developments will focus on evaluating the algorithm's sensitivity and effectiveness by analyzing multiple earthquake events with varying magnitudes. This will help assess the approach's capability in detecting, locating, and quantifying different levels of structural damage. Additionally, further studies aim to enhance the model's ability to predict potential structural failures under diverse seismic conditions.

## REFERENCES

- [1] Masri, S. 1978. "Response of a multidegree-of-freedom system to nonstationary random excitation." *ASME J. Appl. Mech.* 45 (3): 649–656. <https://doi.org/10.1115/1.3424376>.
- [2] Masri, S., G. Bekey, H. Sassi, and T. Caughey. 1982. "Non-parametric identification of a class of non-linear multidegree dynamic systems." *Earthquake Eng. Struct. Dyn.* 10 (1): 1–30. <https://doi.org/10.1002/eqe.4290100102>.
- [3] Masri, S., J. Caffrey, T. Caughey, A. Smyth, and A. Chassiakos. 2004. "Identification of the state equation in complex non-linear systems." *Int. J. Non Linear Mech.* 39 (7): 11–27. [https://doi.org/10.1016/S0020-7462\(03\)00109-4](https://doi.org/10.1016/S0020-7462(03)00109-4).
- [4] Masri, S., and T. Caughey. 1979. "A nonparametric identification technique for nonlinear dynamic problems." *Trans. ASME. J. Appl. Mech.* 46 (2):433–447. <https://doi.org/10.1115/1.3424568>.
- [5] Masri, S., R. Miller, A. Saud, and T. Caughey. 1987a. "Identification of nonlinear vibrating structures: Part I. Formulation." *Trans. ASME. J. Appl. Mech.* 54 (4): 918–922. <https://doi.org/10.1115/1.3173139>.
- [6] Masri, S., R. Miller, A. Saud, and T. Caughey. 1987b. "Identification of nonlinear vibrating structures: Part II—Applications." *J. Appl. Mech. Trans. ASME* 54 (4): 923–929. <https://doi.org/10.1115/1.3173140>.
- [7] Hernandez-Garcia, M., S. Masri, R. Ghanem, E. Figueiredo, and C. Farrar.
- [8] 2010. "An experimental investigation of change detection in uncertain chain-like systems." *J. Sound Vib.* 329 (12): 2395–2409. <https://doi.org/10.1016/j.jsv.2009.12.024>.
- [9] Hernandez-Garcia, M. R. 2014. "Analytical and experimental studies in modeling and monitoring of uncertain nonlinear systems using data driven reduced-order models." Ph.D. thesis, Dept. of Civil and Environmental Engineering, Univ. of Southern California.
- [10] Abdelbarr M, Massari A, Kholer M, Masri S 2020. Decomposition approach for damage detection, localization, and quantification for a 52-story building in downtown Los Angeles. *J Eng Mech.* [https://doi.org/10.1061/\(ASCE\)EM.1943-7889.0001809](https://doi.org/10.1061/(ASCE)EM.1943-7889.0001809).
- [11] James, G., T. G. Carne, and J. P. Lauffer. 1995. "The natural excitation technique (NExT) for modal parameter extraction from operating structures." *Modal Anal. Int. J. Anal. Experimental Modal Anal.* 10 (4):260–277.
- [12] Tomohiko Hatada, Yoshiki Ikeda, Hajime Hagiwara, Yoshihiro Nitta, and Akira Nishitani 2018. "Damage Evaluation Method based on Acceleration Measurement on Some Restricted Floors." *Proceedings of the 16th European Conference on Earthquake Engineering.*
- [13] Doebling, S. W., C. R. Farrar, and M. B. Prime. 1998. "A summary review of vibration-based damage identification methods." *Shock Vib. Digest* 30 (2): 91–105.
- [14] Doebling, S. W., C. R. Farrar, M. B. Prime, and D. W. Shevitz. 1996. *Damage identification and health monitoring of structural and mechanical systems from changes in their vibration characteristics: A literature review.* Los Alamos, NM: Los Alamos National Laboratory.
- [15] Farrar, C. R., and K. Worden. 2007. "An introduction to structural health monitoring." *Philosophical Trans. Royal Soc. London A: Math. Phys. Eng. Sci.* 365 (1851): 303–315. <https://doi.org/10.1098/rsta.2006.1928>.